Joint Waveform Design and Passive Beamforming for RIS-Assisted Dual-Functional Radar-Communication System

Xinyi Wang, *Graduate Student Member, IEEE*, Zesong Fei, *Senior Member, IEEE*, Zhong Zheng, *Member, IEEE*, and Jing Guo, *Member, IEEE*

***Abstract*—Dual-functional radar-communication (DFRC) technique has been viewed as a promising component in the emerging platforms. When synthesizing the desired transmit beampattern, the degrees of freedom of waveform design is limited, which introduces high multi-user interference (MUI), thus degrading the communication performance. Inspired by the applications of the Reconfigurable Intelligent Surface (RIS) in mitigating MUI, in this paper, we investigate joint waveform design and passive beamforming in RIS-assisted DFRC system. We first study the minimization of MUI under the strict beampattern constraint by jointly optimizing DFRC waveform and RIS phase shift matrix. To deal with the coupled variables, we propose an alternating algorithm based on manifold optimization. Subsequently, the trade-off between radar and communication performances is investigated. Simulation results show that for both cases of strict beampattern and trade-off design, with the help of RIS, the system throughput can be significantly improved. Moreover, compared with the scenario where no RIS is employed, the obtained beampattern matches with the target transmit beampattern better.**

***Index Terms*—Dual-functional radar-communication, waveform design, reconfigurable intelligent surface, manifold optimization.**

I. Introduction

Thanks to the potential of integrating radar and communication functionalities, dual-functional radar-communication (DFRC) systems have attracted widespread interest in multiple areas, such as vehicular networks, unmanned aerial vehicle (UAV) communication and sensing, and multi-function radio frequency systems [1]. To support simultaneous information transmission and target detection, numerous works [2]–[4] have devoted the efforts to DFRC waveform design, and studied the trade-off between radar and communication performances. In [3], the authors studied the beamforming design for joint MIMO radar detection and multi-user multiple-input-single-output (MU-MISO) communication. The objective of joint beamforming design is to approach a desired radar beampattern under the constraints of signal-to-interference-plus-noise (SINR) at users and power budget. However, it has been shown in [19] that the difference between the obtained beampattern and the desired one is large when the number of users are much smaller than the number of antennas. By considering the constant-modulus constraints, in [2] and [4], the authors proposed an efficient branch-and-bound algorithm and a manifold optimization based algorithm to design the DFRC waveform, respectively, with the objective of minimizing multi-user interference (MUI) while satisfying the beampattern similarity constraint. As a step further, the authors investigated the range sidelobe control in [5], and developed a first-order descent algorithm to optimize the weighted summation of communication and radar metrics under per-antenna power budget. However, when approaching the desired radar beampattern, the degrees of freedom (DoFs) in designing DFRC waveform are generally constrained; thus, the MUI cannot be mitigated effectively. Therefore, the communication performance of the DFRC waveform under the strict radar beampattern constraint is not satisfying.

Recently, the reconfigurable intelligent surface (RIS), an energy-efficient revolutionary technique [6], has received much attention owing to its potential in mitigating MUI [7]–[9]. In [7], the authors designed a low-complexity method to optimize the passive beamforming vector of the RIS to maximize the minimum SNR/SINR of users in both multicasting and multi-user downlink transmission. In [8], the authors studied robust beamforming and phase shift design for RIS-assisted MU-MISO system under imperfect channel state information, and proposed an alternating optimization based algorithm to minimize the transmit power under the individual outage probability constraints. In [9], the authors exploited both the beamforming gain brought by RIS and high mobility of UAV to improve the system sum-rate, where UAV's trajectory, RIS scheduling, and communication resource allocation were jointly designed. Besides the aforementioned works which concentrated on communication systems, RIS has also been employed to reduce the mutual interference between spectrum sharing MIMO radar and communication systems in [10]. Motivated by these works, we intend to utilize RIS to address the MUI in DFRC systems, which is still an open problem.

In this paper, we incorporate the DFRC system with RIS technique to exploit the potential of RIS in mitigating MUI, which consequently improves communication performance, and provides a better trade-off between radar and communication performance. We first study joint DFRC waveform and RIS phase shift matrix design by enforcing an equality constraint of radar beampattern. Then we relax the beampattern constraint and minimize the weighted sum of MUI and beampattern dissimilarity. For both cases, we propose an alternating algorithm based on manifold optimization. Simulation results show that, by introducing the RIS, the MUI existed in DFRC system can be effectively reduced, thus leading to remarkable higher system throughput. Moreover, RIS can also balance radar and communication performances, making the obtained waveform match the target transmit beampattern better.

Notations: $a, \mathbf{a}, \mathbf{A}$ denote complex scalar value, vector, matrix, respectively; $\mathbb{C}$ denotes the set of complex numbers; $[\cdot]^*$, $[\cdot]^T$, and $[\cdot]^H$ denote the conjugate, transpose and conjugate-transpose operations, respectively; $\|\cdot\|_F$ denotes the Frobenius norm of its argument; $\mathrm{diag}(\cdot)$ denotes the diagonal operation; $\mathrm{Re}\{\cdot\}$ denotes the real part of its argument; $\mathbf{A} \odot \mathbf{B}$ denotes the Hadamard product of $\mathbf{A}$ and $\mathbf{B}$.

II. System Model

We consider the downlink of an RIS-assisted DFRC system that comprises one N-antenna base station (BS), K single-antenna users, and an L-element RIS, as is shown in Fig. 1. The BS is equipped with an N-antenna uniform linear array (ULA), and serves K users with the help of RIS while tracking targets by receiving the echo signals. We assume that the prior location information of the targets has been obtained by radar in the detection phase, which is employed to synthesize the desired beampattern.

Manuscript received December 15, 2020; revised March 17, 2021; accepted April 21, 2021. Date of publication April 26, 2021; date of current version June 9, 2021. This work was supported in part by the National Natural Science Foundation of China under Grant U20B2039 and 61901033, and in part by the Young Talents Supporting Project by China Association for Science and Technology. The work of Zhong Zheng and Jing Guo was supported by the Beijing Institute of Technology Research Fund Program for Young Scholars. The review of this article was coordinated by Dr. Xiaoxiao Wu. *(Corresponding author: Zesong Fei.)*

The authors are with the School of Information and Electronics, Beijing Institute of Technology, Beijing 100081, China (e-mail: bit_wangxy@163.com; feizesong@bit.edu.cn; zhong.zheng@bit.edu.cn; jingguo@bit.edu.cn).

Digital Object Identifier 10.1109/TVT.2021.3075497

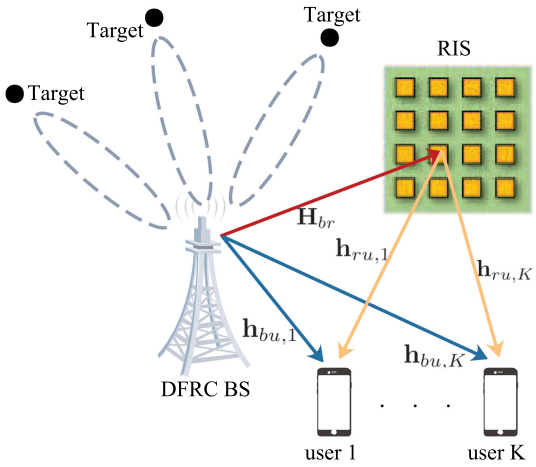

Fig. 1. RIS-assisted DFRC system.

A. MIMO Communication Model

The received signal matrix at the users is given by

$$\mathbf{Y} = (\mathbf{H}_{bu} + \mathbf{H}_{ru}\Theta\mathbf{H}_{br})\mathbf{X} + \mathbf{W} \triangleq \tilde{\mathbf{H}}_{bu}\mathbf{X} + \mathbf{W}, \tag{1}$$

where $\mathbf{H}_{bu} = [\mathbf{h}_{bu,1}, \ldots, \mathbf{h}_{bu,K}]^T \in \mathbb{C}^{K\times N}$, $\mathbf{H}_{ru} = [\mathbf{h}_{ru,1}, \ldots, \mathbf{h}_{ru,K}]^T \in \mathbb{C}^{K\times L}$, $\mathbf{H}_{br} \in \mathbb{C}^{L\times N}$ denote the baseband equivalent channels from BS to users, from RIS to users, and from BS to RIS, respectively. $\mathbf{\Theta} = \mathrm{diag}(\theta_1, \ldots, \theta_L)$ denotes the phase shift matrix of RIS, in which $\theta_l \in \mathcal{F}$, with $\mathcal{F}$ being the feasible of the reflection coefficient at RIS. Here we assume $\mathcal{F} \triangleq \{\theta_l \big| |\theta_l| = 1\}$ [11]. $\mathbf{X} = [\mathbf{x}_1, \ldots, \mathbf{x}_M]$ denotes the transmitted signal matrix, where M is the length of communication frame, and $\mathbf{W} = [\mathbf{w}_1, \ldots, \mathbf{w}_K]^T \in \mathbb{C}^{K\times M}$ is the noise at the users, where $\mathbf{w}_k \sim \mathcal{CN}(0, \sigma^2\mathbf{I}), \forall 1 \le k \le K$. All the channels are assumed to be block-faded and remains unchanged within each frame, and all channels are assumed to be perfectly estimated at BS via pilot symbols.

By denoting the desired symbol matrix at users as $\mathbf{S} \in \mathbb{C}^{K\times M}$, we recast the received signal matrix as

$$\mathbf{Y} = \mathbf{S} + \underbrace{(\tilde{\mathbf{H}}_{bu}\mathbf{X} - \mathbf{S})}_{\text{MUI}} + \mathbf{W}, \tag{2}$$

where the second term represents the multi-user interference (MUI). The total energy of MUI is calculated as

$$P_{\text{MUI}} = \left\| \tilde{\mathbf{H}}_{bu}\mathbf{X} - \mathbf{S} \right\|_F^2, \tag{3}$$

which has a significant impact on the achievable sum-rate of the users. Specifically, the signal-to-interference-plus-noise ratio (SINR) per frame for the k-th user is given as [12]

$$\gamma_k = \frac{\mathbb{E}\left(|s_{k,j}|^2\right)}{\underbrace{\mathbb{E}\left(\left|\tilde{\mathbf{h}}_{bu,k}^T\mathbf{x}_j - s_{k,j}\right|^2\right)}_{\text{MUI energy}} + \sigma^2}, \tag{4}$$

where $\mathbb{E}(\cdot)$ represents the expectation of the argument with respect to j. The achievable sum-rate is then calculated as

$$R = \sum_{k=1}^{K} \log_2(1 + \gamma_k). \tag{5}$$

Note that for a given constellation with fixed energy, the power of desired signal $\mathbb{E}_j(|s_{k,j}|^2)$ is a fixed value. Hence, the achievable data rate of user k can be maximized by minimizing its received interference. In this sense, minimizing MUI energy is closely related to maximizing sum-rate. Therefore, following [2], we adopt the MUI energy as the communication performance metric.

B. MIMO Radar Model

Different from the conventional phased-array radar, a MIMO radar can transmit multiple probing signals that enjoys higher DoFs and waveform diversity [13]. As implied in [2], [13], [14], the beampattern design for MIMO radar is equivalent to the design of the signal covariance matrix, which can be expressed as

$$\mathbf{R}_X = \frac{1}{M}\mathbf{X}\mathbf{X}^H, \tag{6}$$

and the transmit beampattern is given as

$$P_d(\phi) = \mathbf{a}^H(\phi)\,\mathbf{R}_X\,\mathbf{a}(\phi), \tag{7}$$

where ϕ denotes the detection angle, $\mathbf{a}(\phi) = [1, e^{j2\pi\delta\sin(\phi)}, \ldots, e^{j2\pi(N-1)\delta\sin(\phi)}]^T \in \mathbb{C}^{N\times 1}$ is the antenna steering vector with δ denoting the normalized antenna spacing. $P_d(\theta)$ reflects the spatial spectrum of the transmit waveform, which indicates that a larger value of $P_d(\theta)$ results in a larger radiation power towards the direction θ.

III. Joint Waveform and Phase Shift Matrix Design for Given Radar Beampattern

In this section, we firstly recall the beampattern design for colocated MIMO radar, from which a desired radar beampattern is obtained for the design of DFRC waveform. Then we formulate the MUI minimization problem for given radar beampattern by jointly optimizing the DFRC waveform and phase shift matrix of RIS. Subsequently, we propose an alternating optimization based method for solving the formulated problem.

A. Problem Formulation

For the beampattern design of MIMO radar, a constrained least-squares problem is formulated in [3] to approach an ideal beampattern as follows

$$\min_{\beta,\mathbf{R}_d} \sum_{m=1}^{M} \left|\beta\tilde{P}_d(\phi_m) - \mathbf{a}^H(\phi_m)\,\mathbf{R}_d\mathbf{a}(\phi_m)\right|^2 \tag{8}$$

$$\text{s.t. } \mathrm{diag}(\mathbf{R}_d) = \frac{P_0\mathbf{1}}{\sigma^2}, \tag{8a}$$

$$\mathbf{R}_d \succeq 0, \tag{8b}$$

$$\beta \ge 0, \tag{8c}$$

where $\{\phi_k\}_{k=1}^K$ denotes a fine angular grid that covers the detection angle range of $[-\pi/2, \pi/2]$, $\tilde{P}_d(\phi_k)$ is the desired ideal beampattern gain at θ_k, β is a scaling factor, $\mathbf{R}_d$ represents the desired waveform covariance matrix, and P_0 is the power budget. The problem (8) is convex, and β and $\mathbf{R}_d$ can be jointly optimized via existed CVX solvers.

Given a desired covariance matrix $\mathbf{R}_d$, the MUI minimization problem is formulated as

$$\min_{\mathbf{X},\mathbf{\Theta}} \left\| \tilde{\mathbf{H}}_{bu}\mathbf{X} - \mathbf{S} \right\|_F^2 \tag{9}$$

$$\text{s.t.} \quad \frac{1}{M}\mathbf{X}\mathbf{X}^H = \mathbf{R}_d, \tag{9a}$$

$$|\theta_l| = 1, \forall l = 1, \ldots, L, \tag{9b}$$

B. Proposed Algorithm

Since the optimization variables $\mathbf{X}$ and $\mathbf{\Theta}$ are coupled with each other, the problem (9) is challenging to solve, and the optimal solution can hardly be obtained; hence, we propose an alternating optimization based algorithm for jointly designing $\mathbf{X}$ and $\mathbf{\Theta}$.

1) Optimization of $\mathbf{X}$ for Given $\mathbf{\Theta}$: For any given $\mathbf{\Theta}$, problem (9) can be written as

$$\min_{\mathbf{X}} \left\| \tilde{\mathbf{H}}_{bu}\mathbf{X} - \mathbf{S} \right\|_F^2 \tag{10}$$

$$\text{s.t.} \quad \frac{1}{M}\mathbf{X}\mathbf{X}^H = \mathbf{R}_d, \tag{10a}$$

By defining the Cholesky decomposition of $\mathbf{R}_d$ as $\mathbf{R}_d = \mathbf{F}\mathbf{F}^H$, where $\mathbf{F} \in \mathbb{C}^{N\times N}$ is a lower triangular matrix, it has been shown in [2] that the optimal solution of the problem (10) is given as

$$\mathbf{X} = \sqrt{M}\mathbf{F}\tilde{\mathbf{U}}\mathbf{I}_{N\times M}\tilde{\mathbf{V}}^H, \tag{11}$$

where $\tilde{\mathbf{U}}\tilde{\mathbf{\Sigma}}\tilde{\mathbf{V}}^H = \mathbf{F}^H\tilde{\mathbf{H}}_{bu}^H\mathbf{S}$ is the singular value decomposition (SVD) of $\mathbf{F}^H\tilde{\mathbf{H}}_{bu}^H\mathbf{S}$.

2) Optimization of $\mathbf{\Theta}$ for Given $\mathbf{X}$: For any given $\mathbf{X}$, problem (9) can be written as

$$\min_{\mathbf{\Theta}} \left\| \tilde{\mathbf{H}}_{bu}\mathbf{X} - \mathbf{S} \right\|_F^2 \tag{12}$$

$$\text{s.t.} \quad |\theta_l| = 1, \forall l = 1, \ldots, L, \tag{12a}$$

Substituting $\tilde{\mathbf{H}}_{bu}$ in (1) into (12) and removing the terms which are not related with $\mathbf{\Theta}$, we can recast the problem (12) as

$$\min_{\mathbf{\Theta}} \text{Tr}(\mathbf{\Theta}^H\mathbf{B}\mathbf{\Theta}\mathbf{C}) + \text{Tr}(\mathbf{\Theta}^H\mathbf{D}^H) + \text{Tr}(\mathbf{\Theta}\mathbf{D}) \tag{13}$$

$$\text{s.t.} \quad |\theta_l| = 1, \forall l = 1, \ldots, L, \tag{13a}$$

where $\mathbf{B} = \mathbf{H}_{ru}^H\mathbf{H}_{ru}$, $\mathbf{C} = \mathbf{H}_{br}\mathbf{X}\mathbf{X}^H\mathbf{H}_{br}^H$, $\mathbf{D} = \mathbf{H}_{br}\mathbf{X}\mathbf{T}^H\mathbf{H}_{ru}$, and $\mathbf{T} = \mathbf{H}_{bu}\mathbf{X} - \mathbf{S}$.

Furthermore, by defining $\boldsymbol{\theta} = \mathbf{\Theta}\mathbf{1}_L$, we have

$$\text{Tr}(\mathbf{\Theta}^H\mathbf{B}\mathbf{\Theta}\mathbf{C}) = \boldsymbol{\theta}^H(\mathbf{B} \odot \mathbf{C}^T)\boldsymbol{\theta}. \tag{14}$$

Likewise, by defining $\mathbf{d} = [D_{1,1}, \cdot, D_{L,L}]^T$, we have

$$\text{Tr}(\mathbf{\Theta}\mathbf{D}) = \mathbf{d}^T\boldsymbol{\theta}, \text{Tr}(\mathbf{\Theta}^H\mathbf{D}^H) = \boldsymbol{\theta}^H\mathbf{d}^*. \tag{15}$$

By substituting (14) and (15) into (13), problem (13) can be written as

$$\min_{\boldsymbol{\theta}} f(\boldsymbol{\theta}) = \boldsymbol{\theta}^H(\mathbf{B} \odot \mathbf{C})\boldsymbol{\theta} + \mathbf{d}^T\boldsymbol{\theta} + \boldsymbol{\theta}^H\mathbf{d}^* \tag{16}$$

$$\text{s.t.} \quad |\theta_l| = 1, \forall l = 1, \ldots, L, \tag{16a}$$

Problem (16) is still non-convex due to the constraint (16 a). A common technique to tackle this constraint is the semidefinite relaxation (SDR) technique [15]. However, employing SDR may not lead to a unit rank solution, and the approximation methods such as Gaussian randomization cannot guarantee the convergence of the overall algorithm [16]. In what follows, we propose an oblique manifold algorithm to solve this problem.

Algorithm 1: Riemannian Steepest Descent Algorithm for Solving Problem (16).

Input: Convergence threshold ϵ, maximum iteration number.
1: Initialize $\boldsymbol{\theta}_0$ as a feasible solution to the problem (16).
2: Initialize δ as a number larger than ϵ.
3: Set $k = 0$.
4: **repeat**
5: Compute the step size α_k according to [17].
6: Compute Euclidean gradient $\nabla f(\boldsymbol{\theta}_k)$ based on (19).
7: Compute Riemannian gradient $\text{grad}_{\boldsymbol{\theta}_k} f$ based on (20).
8: Update $\boldsymbol{\theta}_{k+1}$ based on (21).
9: Update $k = k + 1$.
10: **until** $\text{grad}_{\boldsymbol{\theta}_k} f \leq \epsilon$ or maximum iteration reached
Output: $\boldsymbol{\theta}$.

Firstly, we note that the constraint defines an oblique manifold [17], which can be characterized by

$$\mathcal{O} = \{\boldsymbol{\theta} \in \mathbb{C}^L | [\boldsymbol{\theta}\boldsymbol{\theta}^H]_{l,l} = 1, \forall l = 1, \ldots, L\}. \tag{17}$$

The *tangent space* of the oblique manifold $\mathcal{O}$ at the point $\boldsymbol{\theta}_i$ is defined as the space which contains all tangent vectors of the oblique manifold $\mathcal{O}$ at $\boldsymbol{\theta}_i$, denoted by $T_{\boldsymbol{\theta}_i}\mathcal{O}$, which can be expressed as

$$T_{\boldsymbol{\theta}_i}\mathcal{O} = \{\mathbf{u} \in \mathbb{C}^L | [\mathbf{u}\boldsymbol{\theta}_i^H]_{l,l} = 0, \forall l = 1, \ldots, L\}, \tag{18}$$

where $\mathbf{u}$ represents a tangent vector at $\boldsymbol{\theta}_i$. The tangent vector that corresponds to the fastest increase of the objective function is defined as the *Riemannian gradient*, and denoted as $\text{grad}_{\boldsymbol{\theta}_i} f$.

To calculate the Riemannian gradient, we first calculate the Euclidean gradient of the objective function (16) as

$$\nabla f(\boldsymbol{\theta}) = 2\left[(\mathbf{B} \odot \mathbf{C})\boldsymbol{\theta} + \mathbf{d}^*\right]. \tag{19}$$

The Riemannian gradient is then obtained by projecting $\nabla f(\boldsymbol{\theta})$ onto the target space $T_{\boldsymbol{\theta}_i}\mathcal{O}$ as [17]

$$\text{grad}_{\boldsymbol{\theta}_i} f = \nabla f(\boldsymbol{\theta}) - \text{Re}\{\nabla f(\boldsymbol{\theta}_i) \odot \boldsymbol{\theta}_i^*\} \odot \boldsymbol{\theta}_i. \tag{20}$$

By applying Riemannian steepest descent (RSD) algorithm, the descent direction at the k-th iteration, ξ_k, is chosen as the negative counterpart of the Riemannian gradient, i.e., $\xi_k = -\text{grad}_{\boldsymbol{\theta}_k}$, and the $\boldsymbol{\theta}$ at the $(k+1)$-th iteration is updated as

$$\boldsymbol{\theta}_{k+1} = R_{\boldsymbol{\theta}_k}(\alpha_k\xi_k), \tag{21}$$

where α_k is the step size, and $R_{\boldsymbol{\theta}} : T_{\boldsymbol{\theta}}\mathcal{O} \to \mathcal{O}$ is called a retraction at the point $\boldsymbol{\theta}$, which maps the tangent space $T_{\boldsymbol{\theta}}\mathcal{O}$ onto $\mathcal{O}$. A typical retraction is stated as [18]

$$R_{\boldsymbol{\theta}_k}(\alpha_k\xi_k) = \left[\frac{(\boldsymbol{\theta}_k + \alpha_k\xi_k)_i}{|(\boldsymbol{\theta}_k + \alpha_k\xi_k)_i|}\right]. \tag{22}$$

Based on the aforementioned Riemannian gradient and retraction operation, we develop a manifold optimization based algorithm for solving Problem (16), as shown in Algorithm 1. Since Algorithm 1 is based on gradient descent, the objective function in (16) is non-increasing in each iteration. Therefore, Algorithm 1 is guaranteed to converge.

3) Overall Algorithm: Based on the aforementioned algorithms, the overall alternating optimization algorithm is summarized in Algorithm 2. Recall that the objective function is monotonically non-increasing in each iteration of both Algorithm 1 and Algorithm 2. Therefore, the

Algorithm 2: Overall Alternating Optimization Algorithm for Solving Problem (9).

Input: Convergence threshold η, maximum iteration number.
1: Initialize $\mathbf{\Theta}_0$ as the identity matrix.
2: Initialize δ as a number larger than ϵ.
3: Set $k = 0$.
4: **repeat**
5: Compute $\mathbf{X}_k$ for given $\mathbf{\Theta}_k$ according to (11).
6: Solve the problem (16) for given $\mathbf{X}_k$ and obtain $\mathbf{\Theta}_{k+1}$.
7: Update $k = k + 1$.
8: **until** the value of objective function (9) converged or maximum iteration reached
Output: $\mathbf{X}$, $\mathbf{\Theta}$.

alternating optimization algorithm is guaranteed to converge. Although it may lead to a sub-optimal solution, we will show its effectiveness via simulation.

In each iteration, the complexity of $\mathbf{X}_k$ is $\mathcal{O}(NM^2 + N^2M + NKM + N^3 + N^2K)$, while the dominated complexity of the optimization of $\mathbf{\Theta}_k$ comes from calculating the gradient, i.e., (19), which is $\mathcal{O}(N^2L)$. Therefore, the total complexity is $\mathcal{O}\{N_{iter,o}(NM^2 + N^2M + NKM + N^3 + N^2K + N_{iter,i}N^2L)\}$, where $N_{iter,o}$ and $N_{iter,i}$ denote the iteration number of outer iterations and inner iterations, respectively.

IV. Joint Design With Trade-Off Between Radar and Communication Performance

As illustrated in [2], since the problem (9) enforces a strict equality constraint of radar beampattern, the communication may suffer from serious performance loss. To address this issue, in this section, we also consider a trade-off between radar and communication performance, i.e., we allow a tolerable mismatch between the designed and desired beampatterns.

A. Problem Formulation

The trade-off optimization problem is formulated as

$$\min_{\mathbf{X},\mathbf{\Theta},\mathbf{U}} \rho \left\| \tilde{\mathbf{H}}_{bu}\mathbf{X} - \mathbf{S} \right\|_F^2 + (1-\rho)\|\mathbf{X} - \mathbf{U}\|_F^2 \tag{23}$$

$$\text{s.t.} \quad \frac{1}{M}\mathbf{U}\mathbf{U}^H = \mathbf{R}_d, \tag{23a}$$

$$\frac{1}{M}\|\mathbf{X}\|_F^2 = P_0, \tag{23b}$$

$$|\theta_l| = 1, \forall l = 1, \ldots, L, \tag{23c}$$

where $\rho \in [0, 1]$ is a given weighting factor that trade-off radar and communication performances, $\mathbf{U}$ is the waveform template that matches the desired radar beampattern, and the constraint (23 b) constrains the total transmission power as the maximum.

B. Alternating Optimization Algorithm

To solve the non-convex problem (23), we propose an alternating optimization based algorithm to iteratively optimize each variable while fixing the other variables.

Algorithm 3: Overall Alternating Optimization Algorithm for Solving Problem (23).

Input: Convergence threshold η, maximum iteration number.
1: Initialize $\mathbf{\Theta}_0$ as the identity matrix.
2: Initialize $\mathbf{U}_0$ as the solution for problem (10).
3: Initialize δ as a number larger than ϵ.
4: Set $k = 0$.
5: **repeat**
6: Solve the problem (24) and obtain $\mathbf{X}_k$ for given $\mathbf{\Theta}_k$ and $\mathbf{U}_k$.
7: Compute $\mathbf{U}_{k+1}$ for given $\mathbf{X}_k$ according to (26).
8: Solve the problem (16) for given $\mathbf{X}_k$ and obtain $\mathbf{\Theta}_{k+1}$.
9: Update $k = k + 1$.
10: **until** the value of objective function (23) converged or maximum iteration reached
Output: $\mathbf{X}$, $\mathbf{\Theta}$, $\mathbf{U}$.

1) Optimization of $\mathbf{X}$ for Given $\mathbf{\Theta}$ and $\mathbf{U}$: We first denote $\mathbf{A} = [\sqrt{\rho}\mathbf{H}^T, \sqrt{1-\rho}\mathbf{I}_N]^T$, $\mathbf{B} = [\sqrt{\rho}\mathbf{S}^T, \sqrt{1-\rho}\mathbf{U}^T]^T$, and reformulate problem (23) as

$$\min_{\mathbf{X}} \|\mathbf{A}\mathbf{X} - \mathbf{B}\|_F^2 \tag{24}$$

$$\text{s.t.} \quad \text{(23b)}$$

Problem (24) can then be solved via the Algorithm 1 in [2].

2) Optimization of $\mathbf{U}$ for Given $\mathbf{\Theta}$ and $\mathbf{X}$: Subsequently, we update the waveform template $\mathbf{U}$, and the problem (23) can be simplified as

$$\min_{\mathbf{U}} \|\mathbf{U} - \mathbf{X}\|_F^2 \quad \text{s.t. (23a)} \tag{25}$$

Similar to (10), the optimal of the problem (25) is given as

$$\mathbf{U} = \sqrt{M}\mathbf{F}\bar{\mathbf{U}}\mathbf{I}_{N\times M}\bar{\mathbf{V}}^H, \tag{26}$$

where $\bar{\mathbf{U}}\bar{\mathbf{\Sigma}}\bar{\mathbf{V}}^H = \mathbf{F}^H\mathbf{X}$ is the singular value decomposition (SVD) of $\mathbf{F}^H\mathbf{X}$.

3) Optimization of $\mathbf{\Theta}$ for Given $\mathbf{X}$ and $\mathbf{U}$: Note that only the first term of the objective (23) is related to $\mathbf{\Theta}$. Therefore, the optimization algorithm for $\mathbf{\Theta}$ is the same as that in Section III.

4) Overall Algorithm: Based on the aforementioned algorithms, the overall algorithm is summarized in Algorithm 3. According to [2], the complexity of optimizing $\mathbf{X}$ is in the same order of that of optimizing $\mathbf{U}$. Therefore, the complexity of Algorithm 3 is also $\mathcal{O}\{N_{iter,o}(NM^2 + N^2M + NKM + N^3 + N^2K + N_{iter,i}N^2L)\}$.

V. Simulation Results

In this section, we validate the proposed joint waveform and RIS reflecting matrix design algorithms via numerical results. Following the assumption in [2], each entry of the channel matrix subject to standard Complex Gaussian distribution. The antenna number of BS is set to be $N = 20$, and the total power budget is set as $P_0 = 20$ dBm. The transmit SNR is defined as SNR $= P_0/N_0$. The cases of strict beampattern equality constraint and trade-off design are denoted as 'Strict' and 'Trade-off,' respectively. We also compared the results with no aid of RIS [2]. We assume three targets are located at the angles of $[-60°, 0°, 60°]$ with respect to the BS, respectively. Note that we assume that the angles are obtained by the BS in the detection phase and utilized to design ideal beampattern.

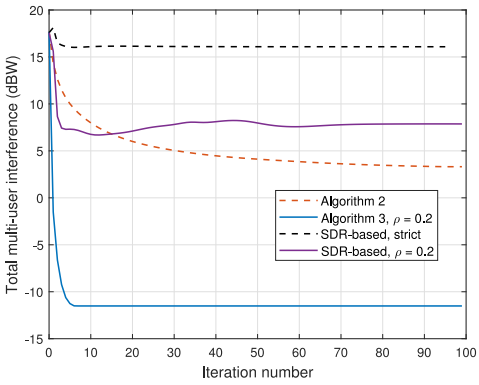

Fig. 2. Convergence performance of the proposed algorithms.

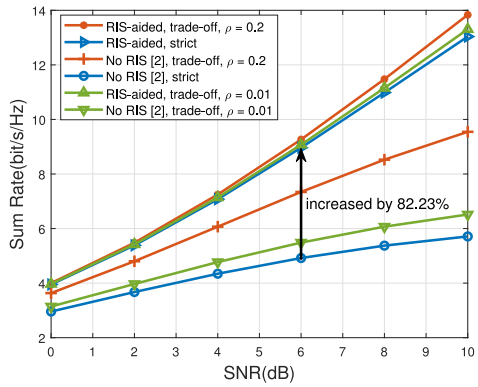

(a)

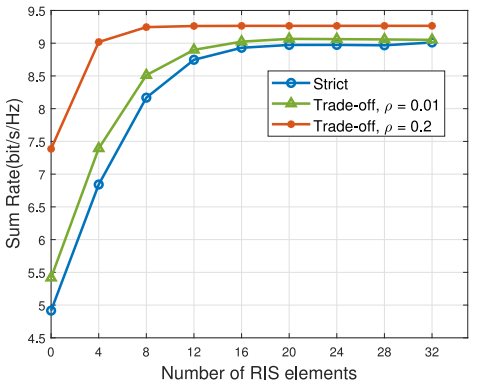

(b)

Fig. 3. (a) Sum rate vs. Transmit SNR, $L = 16$. (b) Sum rate vs. number of RIS elements L, SNR $= 6$ dB.

In Fig. 2, we present the convergence behaviours of the proposed Algorithm 2 and Algorithm 3. As can be seen, compared with Algorithm 2, Algorithm 3 converges faster. The reason is that, by allowing the dissimilarity between optimized and desired beampatterns, more DoFs are introduced in each iteration; thus, the convergence is achieved more quickly. In addition, we also present the performance of the SDR-based approach. Due to the rank-one approximation in SDR technique, the SDR-based algorithm cannot converge and results in a larger objective value. The comparison with SDR-based approach also shows the superiority of our proposed algorithms.

In Fig. 3(a), we show the sum rates achieved by different approaches with different transmit SNRs, where $L = 16$. It shows that, with the aid of RIS, the sum rate can be remarkably improved, for both cases of strict beampattern constraint and trade-off design. Meanwhile, with the weighting factor ρ increasing, the sum rate also increases at the expense of mismatching between optimized and desired beampatterns. Fig. 3(b) shows the sum rates with different RIS elements, where transmit SNR is set as 6 dB. As can be seen, the sum rates of all approaches increase with the increasing of L, while the differences among them decrease. Finally, the achieved sum rates of all approaches converge with a sufficient large RIS element number. It is also noteworthy that the performance gain of improving ρ is lower when utilizing RIS. The reason is that, by jointly designing waveform and RIS reflecting matrix, the BS-user channel and waveform can match with each other better. Therefore, trade-off between radar and communication performances is decreased.

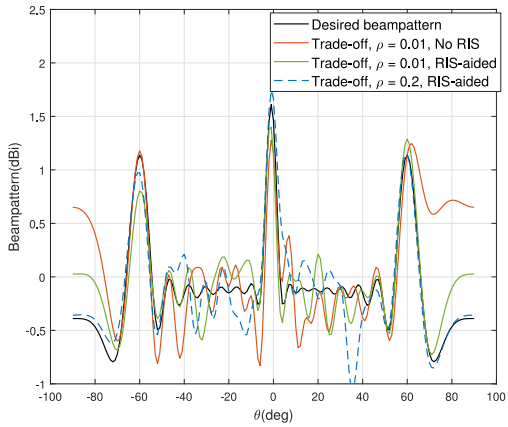

(a)

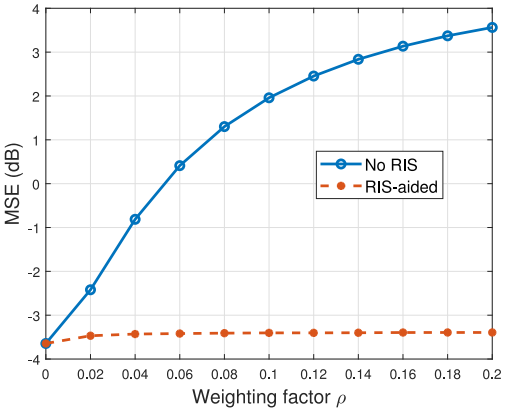

(b)

Fig. 4. (a) Radar beampatterns with different approaches, $N = 20$, $K = 4$. (b) MSE of the obtained beampattern, $N = 20$, $K = 4$.

In Fig. 4(a), we present the resultant radar beampatterns. The beampattern for 'Strict' approach is the same with the desired beampattern. By introducing a small weighting factor $\rho = 0.01$, the beampattern of [2], where no RIS is exploited, degrades seriously. While for RIS-assisted approach, the designed beampattern matches the desired one well. This is because RIS is able to help decrease MUI to a slight value; thus, the objective of solving problem (23) is approximated as minimizing the dissimilarity between the designed and desired waveforms. To make it more clarified, we present the mean square error (MSE) of the obtained beampattern in Fig. 4(b). As can be seen, compared with the case where no RIS is employed, the MSE can be remarkably reduced. The results in Fig. 4 together with those in Fig. 3(a)

and Fig. 3(b) indicate that RIS is able to help achieve a better balance between radar and communication performances.

VI. Conclusion

In this paper, we studied joint waveform design and passive beamforming for RIS-assisted DFRC systems. For both strict radar beampattern constraint and trade-off between radar and communication performances, we proposed an alternating algorithm based on manifold optimization to jointly design DFRC waveform and RIS phase shift matrix. Simulation results validated the effectiveness of RIS in mitigating MUI and balancing radar and communication performances.

References

[1] F. Liu, C. Masouros, A. P. Petropulu, H. Griffiths, and L. Hanzo, "Joint radar and communication design: Applications, state-of-the-art, and the road ahead," *IEEE Trans. Commun.*, vol. 68, no. 6, pp. 3834–3862, Jun. 2020.

[2] F. Liu, L. Zhou, C. Masouros, A. Li, W. Luo, and A. Petropulu, "Toward dual-functional radar-communication systems: Optimal waveform design," *IEEE Trans. Signal Process.*, vol. 66, no. 16, pp. 4264–4279, Aug. 2018.

[3] F. Liu, C. Masouros, A. Li, H. Sun, and L. Hanzo, "MU-MIMO communications with MIMO radar: From co-existence to joint transmission," *IEEE Trans. Wireless Commun.*, vol. 17, no. 4, pp. 2755–2770, Apr. 2018.

[4] F. Liu, C. Masouros, and H. Griffiths, "Dual-functional radar-communication waveform design under constant-modulus and orthogonality constraints," in *Proc. Sensor Signal Process. Defence Conf.*, 2019, pp. 1–5.

[5] F. Liu, C. Masouros, T. Ratnarajah, and A. Petropulu, "On range sidelobe reduction for dual-functional radar-communication waveforms," *IEEE Wireless Commun. Lett.*, vol. 9, no. 9, pp. 1572–1576, Sep. 2020.

[6] J. Zhang, E. Bjornson, M. Matthaiou, D. W. K. Ng, H. Yang, and D. J. Love, "Prospective multiple antenna technologies for beyond 5G," *IEEE J. Sel. Areas Commun.*, vol. 38, no. 8, pp. 1637–1660, Aug. 2020.

[7] K. Huang and H. Wang, "Passive beamforming for IRS aided wireless networks," *IEEE Wireless Commun. Lett.*, vol. 9, no. 12, pp. 2035–2039, Dec. 2020.

[8] J. Wang, Y. Liang, S. Han, and Y. Pei, "Robust beamforming and phase shift design for IRS-enhanced multi-user MISO downlink communication," *Proc. ICC 2020-2020 IEEE Int. Conf. Commun.*, 2020, pp. 1–6.

[9] Z. Wei *et al.*, "Sum-rate maximization for IRS-assisted UAV OFDMA communication systems," *IEEE Trans. Wireless Commun.*, vol. 20, no. 4, pp. 2530–2550, Apr. 2021.

[10] X. Wang, Z. Fei, J. Guo, Z. Zheng, and B. Li, "RIS-assisted spectrum sharing between MIMO radar and MU-MISO communication systems," *IEEE Wireless Commun. Lett.*, vol. 10, no. 3, pp. 594–598, Mar. 2021.

[11] X. Meng, F. Liu, J. Zhou, and S. Yang, "Interference exploitation precoding for intelligent reflecting surface aided communication system," *IEEE Wireless Commun. Lett.*, vol. 10, no. 1, pp. 126–130, Jan. 2021.

[12] S. K. Mohammed and E. G. Larsson, "Per-antenna constant envelope precoding for large multi-user MIMO systems," *IEEE Trans. Commun.*, vol. 61, no. 3, pp. 1059–1071, Mar. 2013.

[13] J. Li and P. Stoica, "MIMO radar with colocated antennas," *IEEE Signal Process. Mag.*, vol. 24, no. 5, pp. 106–114, Sep. 2007.

[14] D. R. Fuhrmann and G. S. Antonio, "Transmit beamforming for MIMO radar systems using signal cross-correlation," *IEEE Trans. Aerosp. Electron. Syst.*, vol. 44, no. 1, pp. 171–186, Jan. 2008.

[15] Z. Luo, W. Ma, A. M. So, Y. Ye, and S. Zhang, "Semidefinite relaxation of quadratic optimization problems," *IEEE Signal Process. Mag.*, vol. 27, no. 3, pp. 20–34, May 2010.

[16] J. C. Bezdek and R. J. Hathaway, "Some notes on alternating optimization," in *Proc. AFSS Int. Conf. Fuzzy Syst.*, 2002, pp. 288–300.

[17] P. A. Absil, R. Mahony, and R. Sepulchre, *Optimization Algorithms on Matrix Manifolds*. Princeton, NJ, USA: Princeton Univ. Press, 2009.

[18] X. Yu, J. Shen, J. Zhang, and K. B. Letaief, "Alternating minimization algorithms for hybrid precoding in millimeter wave MIMO systems," *IEEE J. Sel. Topics Signal Process.*, vol. 10, no. 3, pp. 485–500, Apr. 2016.

[19] X. Liu, T. Huang, N. Shlezinger, Y. Liu, J. Zhou, and Y. C. Eldar, "Joint transmit beamforming for multiuser MIMO communications and MIMO radar," *IEEE Trans. Signal Process.*, vol. 68, pp. 3929–3944, 2020.